

贵州道坨锰矿成矿时代及环境的 Re-Os 同位素证据

裴浩翔^{1,2}, 付勇^{3,1*}, 李超⁴, 李延河^{1,2}, 安正泽⁵

1. 中国地质科学院矿产资源研究所, 北京 100037;
2. 国土资源部成矿作用与资源评价重点实验室, 北京 100037;
3. 贵州大学资源与环境工程学院, 贵阳 550000;
4. 国家地质实验测试中心, 北京 100037;
5. 贵州省地质矿产勘查开发局一〇三地质大队, 铜仁 554300

* 联系人, E-mail: byez1225@126.com

2017-04-26 收稿, 2017-07-19 修回, 2017-07-20 接受, 2017-09-15 网络版发表

国家自然科学基金(41472089)和中国地质调查局地质调查项目(DD20160346)资助

摘要 2010年发现的贵州道坨锰矿是一个超大型的海相沉积矿床, 其含矿地层为南华系大塘坡组一段黑色页岩。对道坨锰矿大塘坡组一段含锰黑色页岩测定的Re-Os同位素等时线年龄为 660.6 ± 7.5 Ma, 该年龄与前人测定的大塘坡组黑色页岩底部凝灰岩夹层中锆石U-Pb年龄在误差范围内一致, 进一步限定了“大塘坡”式锰矿的成矿时代和Sturtian冰期的结束年龄, 且可与全球Sturtian冰期结束的Re-Os同位素年龄进行对比。由Re-Os等时线年龄得到的 $^{187}\text{Os}/^{188}\text{Os}$ 初始比值为0.781, 结合前人的研究成果, 说明在Sturtian冰期后伴随着大气氧含量的快速升高及陆地冰川的融化, 冰川融水携带着陆源物质进入到含Mn²⁺的裂谷盆地, 使得盆地表层水体含氧量迅速增加, 生物大量繁殖, Mn²⁺被氧化为MnO₂而沉淀, 之后在盆地底部还原环境中伴随着有机质的埋藏及成岩作用而最终形成菱锰矿。

关键词 锰矿, 大塘坡组, Re-Os 同位素, 冰期

新元古代是地球演化过程中的重要时期。它是地球由缺氧、生物贫瘠的中元古代向富氧与生物爆发的显生宙转折的时期。在这个时期, 地球上发生了超大陆裂解、雪球地球事件等重大地质事件^[1~4], 这些事件与当时的海水、气候、板块构造运动等多个重大科学问题有关, 近年来一直是地球科学的研究热点。从全球范围看, 在新元古代至少发生了2次全球性的冰川事件, 分别为Sturtian冰期和Marino冰期。在我国扬子地区, 其分别对应着江口冰期和南沱冰期^[5], 在这两个冰期之间的是大塘坡间冰期, 是我国重要的成锰期。

扬子地区南华系的大塘坡组黑色页岩(及相当地层)广泛分布于贵州、湖南、湖北、重庆等地, 在此

层位曾先后发现了贵州大塘坡、西溪堡, 湖南花垣民乐, 重庆秀山等多个大中型锰矿, 因此是我国沉积型锰矿重要的赋矿地层。2010年在此层位发现的贵州道坨锰矿是一个超大型海相沉积型锰矿床, 其成矿时代受大塘坡组地层年龄约束。

目前关于沉积矿床直接定年的方法还比较有限, 一些传统的同位素体系如Rb-Sr, K-Ar, Sm-Nd法由于自身的性质, 不适合对黑色页岩型矿床进行有效的定年。当今被广泛运用的定年手段是凝灰岩中的锆石U-Pb法, 但由于很多地区缺乏相应的测试对象而存在着应用的局限性。近年来, 随着分析测试技术的提高, Re-Os同位素体系作为一种强有力的定年及示踪工具已在金属矿床研究中得到了广泛应用^[6], 且随

引用格式: 裴浩翔, 付勇, 李超, 等. 贵州道坨锰矿成矿时代及环境的 Re-Os 同位素证据. 科学通报, 2017, 62: 3346–3355

Pei H X, Fu Y, Li C, et al. Mineralization age and metallogenic environment of Daotuo manganese deposits in Guizhou: Evidence from Re-Os isotopes (in Chinese). Chin Sci Bull, 2017, 62: 3346–3355, doi: 10.1360/N972017-00450

着研究的深入, Re和Os的“亲有机性”逐渐被广泛关注, 并被应用于富有机质沉积岩的定年及古环境反演中^[7]。黑色页岩形成于富有机质的还原环境, 含有较高含量的¹⁸⁷Re, 这使得其适合于Re-Os同位素体系定年, 其不但能够提供可靠的年龄数据, 还能够通过¹⁸⁷Os/¹⁸⁸Os的初始比值进行有效的示踪^[8~15]。因此本文尝试通过对采自道坨锰矿大塘坡组底部的黑色页岩进行Re-Os同位素分析, 确定大塘坡组黑色页岩的年龄, 为扬子地区提供新的地层对比依据, 并探讨锰矿的形成环境。

1 地质背景

道坨锰矿所处的黔湘渝毗邻区为我国锰矿的集中分布区, 区内已发现贵州大塘坡、西溪堡、杨家湾、黑水溪等多个大中型锰矿。区域所处大地构造位置为江南造山带与扬子陆块过渡区的裂谷带(图1(a))。820 Ma左右, 全球性的大陆裂谷作用使得Rodinia超大陆发生裂解, 在此背景下, 扬子陆块与华夏陆块发生多次拼合与拉张运动, 形成了南华裂谷盆地, 并在盆地之内又形成了一系列的次级裂谷盆地^[18]。在江口冰期结束后的大塘坡期, 沿北东向分布的沉积盆地内沉积了黑色炭质页岩建造, 锰矿即赋存于这些黑色页岩中(图1(b))。

贵州道坨锰矿位于扬子陆块东南边缘与江南造

山带的结合部位, 区域内断裂构造复杂, 褶曲较简单, 主要构造线呈NE, NNE及NEE向展布, 矿区主要受木耳断裂及冷水断裂带控制。区内主要出露青白口系清水江组, 南华系铁丝坳组、大塘坡组和南沱组, 震旦系陡山沱组和留茶坡组, 以及寒武系九门冲组、变马冲组和杷榔组地层(图1(c))。铁丝坳组为一套含砾砂岩及粉砂岩组合, 黄铁矿颗粒较发育, 从下到上颜色逐渐变深, 砾石成分减少, 在与大塘坡组过渡段为灰色、深灰色细粒粉砂岩, 粉砂质页岩, 代表了江口冰期的沉积产物, 与上覆大塘坡组为整合接触。大塘坡组为含锰黑色页岩-黑色页岩-砂岩粉砂岩组合, 从下至上可分为3段(图2(a))。含锰层在大塘坡组一段, 为含锰黑色页岩, 可见浸染状、粒状黄铁矿, 含锰矿物主要为菱锰矿(图2(b)~(g)), 呈层状、透镜状产出, 局部可见方解石细脉。锰含量最高可达40%, 从底部向上逐渐减少, 至一段上部, 小于1%。二、三段为灰色粉砂质页岩, 粉砂岩, 至南沱组逐渐过渡为灰绿色含砾砂岩、砾岩。

2 样品处理

2.1 样品描述

对富有机质沉积岩进行准确的Re-Os同位素分析需要注意样品封闭性, 沉积的同时性, 溶解的单一性

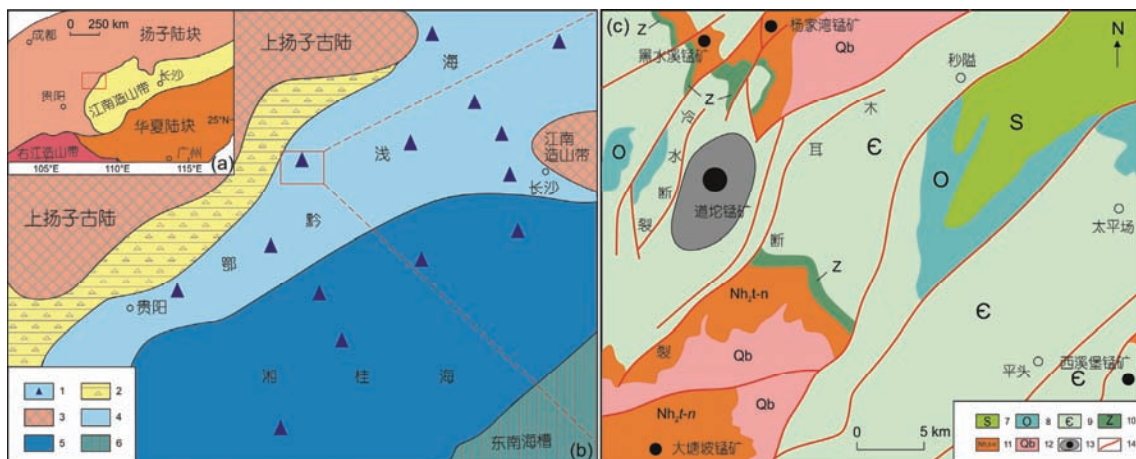


图1 研究区地质背景. (a) 大地构造简图^[16]; (b) 黔东北大塘坡世岩相古地理图^[16]; (c) 道坨锰矿区域地质简图^[17]. 1, 冰水沉积物与暗色泥岩; 2, 古陆冰碛岩; 3, 古陆; 4, 浅海相; 5, 深海相; 6, 海槽; 7, 志留系; 8, 奥陶系; 9, 寒武系; 10, 震旦系; 11, 南华系-铁丝坳组、大塘坡组、南沱组; 12, 青白口系; 13, 矿区及锰床; 14, 断层

Figure 1 Geological background of study area. (a) Tectonic sketch map^[16]; (b) lithofacies palaeogeography map of manganese ore deposits in the northeast of Guizhou Province^[16]; (c) geological map of daotuo manganese deposit^[17]. 1, Fluvio-glacial deposit and dark mudstone; 2, old land tillite; 3, old land; 4, neritic facies; 5, abyssal facies; 6, trough; 7, Silurian; 8, Ordovician; 9, Cambrian; 10, Sinian; 11, Nanhuan-Tiesiao Formation, Datangpo Formation, Nantuo Formation; 12, Qingbaikou; 13, manganese deposit; 14, fault

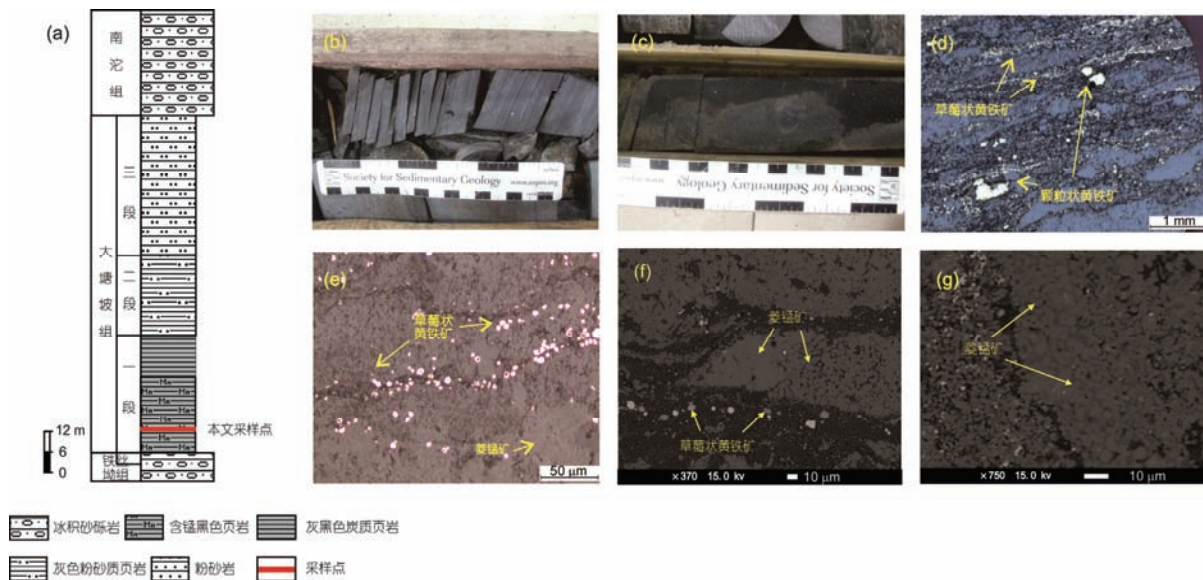


图2 采样位置及样品特征. (a) 道坨锰矿柱状简图及采样点位置; (b) 条带状菱锰矿; (c) 块状菱锰矿; (d), (e) 显微镜下呈层状的草莓状黄铁矿, 分散的颗粒状黄铁矿, 微粒状菱锰矿; (f), (g) 菱锰矿及草莓状黄铁矿的电子探针照片

Figure 2 Sampling position and sample characteristics. (a) Stratigraphic column of Daotuo manganese deposit and sample location; (b) striped rhodochrosite; (c) massive rhodochrosite; (d), (e) microscope images for pyrite framboids, granular pyrite and micro-granular rhodochlorite; (f), (g) ion microprobe images for the rhodochrosite and pyrite framboids

等问题^[7]. 本文中道坨锰矿样品采自ZK102钻孔, 所取样品为铁丝坳组与大塘坡组界线之上约5 m处没有脉体填充的含锰黑色页岩, 所选样品均取自长约几十厘米范围内, 之后用氧化锆球磨机碎至200目待处理. 这既能保证样品Re-Os同位素体系的封闭, 也能够保证样品的近等时性. 关于溶样试剂的选择, 目前国外较多的采用CrO₃-H₂SO₄来处理富有机质沉积岩样品, 认为HCl-HNO₃的氧化性太强, 会将陆源碎屑物质中的Re, Os溶解, 影响数据的准确性^[19]. 但限于国内的试剂纯化水平, CrO₃-H₂SO₄较难纯化, 使得实验流程空白较高, 且在纯化过程中会产生大量含铬废液污染环境, 因此目前国内仍主要采用HCl-HNO₃来溶样^[20,21]. 此外, 条件实验显示, 对于含碎屑少的黑色页岩, HCl-HNO₃溶样和CrO₃-H₂SO₄溶样所得到的Re, Os含量和同位素年龄在误差范围内是一致的^[22]. 而本文所采的大塘坡组含锰页岩形成于较深的裂谷盆地内, 所含陆源碎屑物质较少, 从结果来看, HCl-HNO₃试剂能够将该黑色页岩样品中赋存于有机物中的Re, Os释放出来, 而不溶或很少溶解陆源碎屑物质中的Re和Os^[7,23,24].

2.2 样品分析及测试结果

准确称取0.2 g待分析黑色页岩样品于Carius管

中, 先加入约3 mL经二次蒸馏纯化的10 mol/L HCl, 待反应片刻后, 在液氮冰冻条件下, 加入5 mL经二次蒸馏纯化16 mol/L HNO₃和1 mL 12 mol/L HCl及¹⁸⁵Re和¹⁹⁰Os混合稀释剂, 封口放入不锈钢套管, 并将套管放于烘箱内, 逐渐升温到230℃加热24 h. 将同位素交换平衡后的样品溶液采用蒸馏吸收法分离富集Os, 丙酮萃取法分离纯化Re, 用N-TIMS方法测定Re, Os同位素比值^[13,14,23-26].

道坨矿区10件含锰黑色页岩样品Re的含量为0.26~45.27 ng/g, Os的含量为0.083~0.677 ng/g, ¹⁸⁷Re/¹⁸⁸Os为14.36~807.63, ¹⁸⁷Os/¹⁸⁸Os为0.94~9.71(表1). 通过Isoplot软件所得到的等时线年龄为660.6±7.5 Ma (2σ, n=10, MSWD=24, ¹⁸⁷Os/¹⁸⁸Os=0.781±0.035)(图3).

3 讨论

3.1 锰矿时代及全球Sturtian冰期地层对比

Re, Os元素所具有的亲铜和亲铁特性, 使其成为研究矿床成矿物质来源及判断成矿年代强有力地球化学工具. 而近年来随着分析测试技术的提高, Re-Os同位素体系也逐渐被应用在富有机质沉积岩的定年及古海洋和古环境反演方面. Re, Os一般是以可溶性高价氧化物的形式存在于海水中, 被还原后会

表1 道坨锰矿样品分析结果

Table 1 Results of sample analysis of Daotuo manganese ore

| 样品编号 | Re (ng/g) | | 普 Os (ng/g) | | ^{187}Os (ng/g) | | $^{187}\text{Re}/^{188}\text{Os}$ | | $^{187}\text{Os}/^{188}\text{Os}$ | |
|------------|-----------|------|-------------|-------|--------------------------|--------|-----------------------------------|------|-----------------------------------|------|
| | 测定值 | 不确定度 | 测定值 | 不确定度 | 测定值 | 不确定度 | 测定值 | 不确定度 | 测定值 | 不确定度 |
| ZK102-5-1 | 7.62 | 0.06 | 0.245 | 0.002 | 0.073 | 0.0006 | 209.96 | 2.19 | 3.22 | 0.02 |
| ZK102-5-2 | 31.09 | 0.23 | 0.418 | 0.003 | 0.235 | 0.0017 | 807.63 | 8.24 | 9.71 | 0.01 |
| ZK102-5-3 | 36.23 | 0.27 | 0.51 | 0.004 | 0.279 | 0.0021 | 740.41 | 7.85 | 9.07 | 0.03 |
| ZK102-5-4 | 45.27 | 0.33 | 0.677 | 0.005 | 0.347 | 0.0025 | 650.9 | 6.58 | 7.95 | 0.01 |
| ZK102-5-5 | 0.26 | 0.05 | 0.101 | 0.001 | 0.011 | 0.0001 | 14.36 | 0.15 | 0.95 | 0.01 |
| ZK102-5-6 | 0.27 | 0.08 | 0.098 | 0.001 | 0.017 | 0.0001 | 14.67 | 0.15 | 0.94 | 0.02 |
| ZK102-5-7 | 0.80 | 0.01 | 0.089 | 0.001 | 0.013 | 0.0001 | 49.64 | 0.5 | 1.31 | 0.01 |
| ZK102-5-8 | 0.34 | 0.07 | 0.102 | 0.001 | 0.011 | 0.0001 | 18.17 | 0.19 | 0.96 | 0.03 |
| ZK102-5-9 | 0.27 | 0.09 | 0.083 | 0.001 | 0.01 | 0.0001 | 17.33 | 0.18 | 0.97 | 0.02 |
| ZK102-5-10 | 0.35 | 0.05 | 0.109 | 0.001 | 0.013 | 0.0001 | 17.11 | 0.18 | 0.97 | 0.01 |

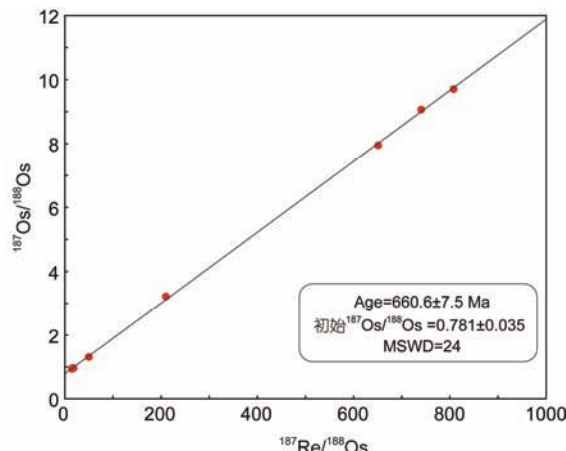


图3 道坨锰矿含锰黑色页岩Re-Os等时线年龄图

Figure 3 Re-Os isochron age of manganese black shale of Daotuo manganese deposit

形成较难迁移的离子，被有机质吸附富集于沉积物中，海水还原度越高，其沉积物中Re, Os的含量相对越高。同时，Re, Os同位素体系的建立与沉积作用具有等时性^[11]，在还原环境中，Re-Os同位素体系是封闭的，后期成岩作用不易使其发生同位素分馏^[27]，因此黑色页岩中的Re-Os同位素体系能够保持其形成过程中的原始信息，其Re-Os等时线年龄能够代表黑色页岩的沉积年龄。本文对道坨锰矿含锰黑色页岩进行的Re-Os同位素定年所得年龄为 660.6 ± 7.5 Ma，该年龄与前人得到的大塘坡组底部的凝灰岩中锆石年龄 662.9 ± 4.3 ^[28]和 667.3 ± 9.9 Ma^[29]在误差范围内是一致的。因此锰矿的形成年龄应该在660 Ma左右，该年龄也有效地约束了铁丝坳冰期的上限年龄，并

可与全球Sturtian冰期后的沉积岩Re-Os同位素年龄进行对比(表2和图4)。

根据最新的国际地层表^[36]，成冰系底界年龄为720 Ma，而关于南华系底界的年龄一直存在着不同认识。最近的研究^[5]为确定南华系底界年龄提供了新的数据，在广西桂北三江盆地丹洲群拱洞组地层(长安组之下)发现的凝灰岩中的锆石年龄为 715.9 ± 2.8 Ma^[35]，这与阿曼的Ghubrah组的火山凝灰岩及加拿大西北部Mackenzie山脉Mount Harper上部冰碛岩内部火山杂岩的年龄 717.6 Ma^[37]在误差范围内是一致，接近于国际地层表的年龄。此外，赞比亚Grand冰砾岩之下的Mwashya组的Re-Os年龄为 727.3 ± 4.9 Ma，虽略早于国际地层表的年龄，但也约束了国际上Sturtian冰期的下限年龄。

3.2 扬子地区Sturtian冰期后古海水Os同位素构成

黑色页岩中Os主要来自于海水，而海水中的Os同位素主要受到3个方面物源的影响：(1)淡水河流带入的较高放射性的Os($^{187}\text{Os}/^{188}\text{Os}$: 0.3~1.26)^[38]；(2)由洋中脊热液带来的Os，具有非放射性成因特征， $^{187}\text{Os}/^{188}\text{Os}$ 约为0.12^[39]；(3)由宇宙尘埃带来的Os，比值接近于地幔值约为0.12^[40]。海水中的Os同位素是三项来源的汇合，不同的地质事件影响Os同位素不同端元的供给，能够很明显地反映在海水的Os同位素变化上，其比值会随着不同时代沉积环境的不同而改变^[7]。目前正常海水 $^{187}\text{Os}/^{188}\text{Os}$ 为 $1.05\sim1.06$ ^[41]，体现了当前环境下的稳定状态，也是讨论地质问题的一个普遍参考。运用Os同位素的比值能够很好地

表2 全球Sturtian/Marinoan冰期时限汇总表

Table 2 The summary of Sturtian/Marinoan glaciations of the world

| 国家或地区 | 地层 | 岩性 | 年龄(Ma) | 测试方法 | $^{187}\text{Os}/^{188}\text{Os}$ 初始值 | 参考文献 |
|-------|----------------|-------|-----------------|-------|---------------------------------------|------|
| 加拿大 | Sheepbed组 | 炭质页岩 | 632.3 ± 3.5 | Re-Os | 1.21 ± 0.04 | [30] |
| 澳大利亚 | Tindelpina组 | 页岩 | 643.0 ± 2.4 | Re-Os | 0.95 ± 0.01 | [31] |
| 澳大利亚 | Aralka组 | 黑色页岩 | 657.2 ± 5.4 | Re-Os | 0.82 ± 0.03 | [31] |
| 蒙古 | Taishir组 | 碳酸盐岩 | 659.0 ± 4.5 | Re-Os | 0.60 ± 0.01 | [30] |
| 苏格兰 | Ballachulish组 | 板岩 | 659.6 ± 9.6 | Re-Os | 1.04 ± 0.03 | [32] |
| 贵州松桃 | 大塘坡组 | 黑色页岩 | 660.6 ± 7.5 | Re-Os | 0.781 ± 0.035 | 本文 |
| 加拿大 | Twitya组 | 黑色页岩 | 662.4 ± 3.9 | Re-Os | 0.54 ± 0.01 | [33] |
| 贵州铜仁 | 大塘坡组 | 凝灰岩锆石 | 662.9 ± 4.3 | U-Pb | 无 | [28] |
| 广西三江 | 长安组 | 凝灰岩锆石 | 716.1 ± 3.4 | U-Pb | 无 | [35] |
| 赞比亚 | Mwashya组 | 页岩 | 727.3 ± 4.9 | Re-Os | 0.35 ± 0.03 | [30] |
| 加拿大 | Coppercap组 | 页岩 | 732.2 ± 3.9 | Re-Os | 0.15 ± 0.002 | [33] |
| 加拿大 | Callison Lake组 | 页岩 | 739.9 ± 6.1 | Re-Os | 0.609 ± 0.01 | [34] |

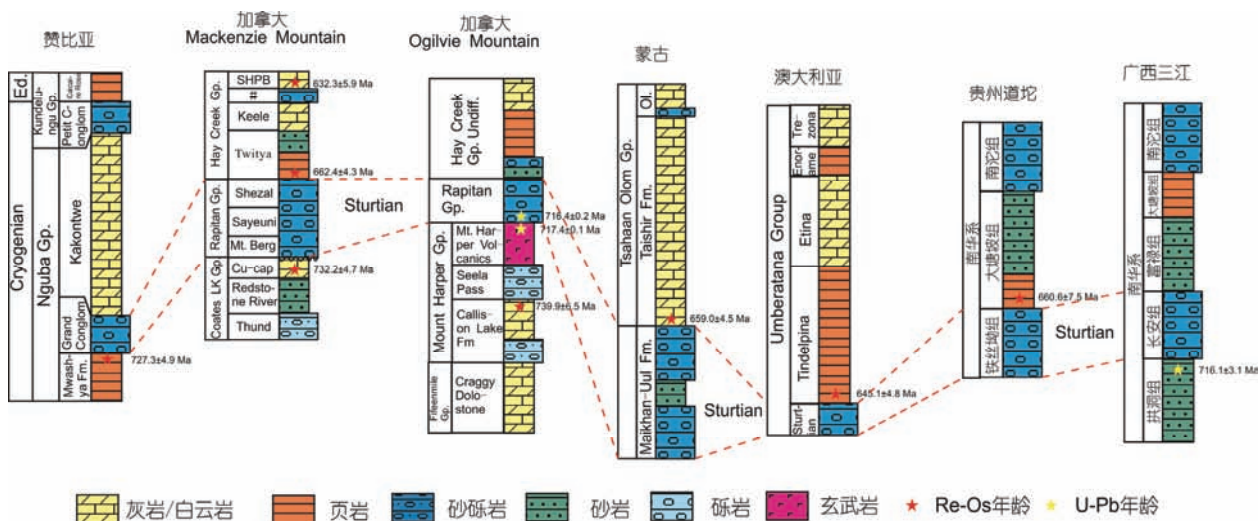


图4 全球Sturtian冰期典型剖面对比图(数据来自表2)

Figure 4 The comparison of typical section of Sturtian glaciation in the world (data from Table 2)

示踪古海洋和古气候环境,如Hannah等人^[42]通过对南非古元古代间冰期海相黑色页岩中的黄铁矿进行Re-Os定年并得到其 $^{187}\text{Os}/^{188}\text{Os}$ 初始值为0.11,该值远小于现代海水Os同位素比值,更接近大洋中脊的热液值,说明古元古代冰期事件期间大陆氧化风化作用基本上没有,海水主要受到海底热液的影响,表现为低 $^{187}\text{Os}/^{188}\text{Os}$ 初始值。同样伴随地幔柱活动所产生的大陆溢流岩浆事件,如65 Ma德干高原玄武岩、中二叠末期峨眉山玄武岩溢流事件都控制着当时大洋中的Os同位素的构成^[10]。Singh等人^[43]对喜马拉雅地区寒武纪黑色页岩进行Re-Os定年研究,得出初始比值为1.18,高于目前海水的比值,说明当时环境下,

喜马拉雅地区大陆风化作用比目前的大陆风化作用更高更强,能够使更多放射性成因Os进入大洋,形成高于现代海水的Os同位素的组成。

根据Re-Os同位素体系的基本原理,本文从大塘坡组黑色页岩的等时线年龄所得到的Os同位素初始值代表了该地区大塘坡时期古海水的Os同位素组成,其 $^{187}\text{Os}/^{188}\text{Os}$ 初始值为0.781,该值明显小于目前正常海水的值,体现了当时大气和海水环境的一个平衡。从全球新元古代地层来看,尚没有Sturtian冰期期间时海水的 $^{187}\text{Os}/^{188}\text{Os}$ 数据。但从目前得到的冰期前后页岩的 $^{187}\text{Os}/^{188}\text{Os}$ 初始值可以看出,在Sturtian冰期前, $^{187}\text{Os}/^{188}\text{Os}$ 初始值为0.1~0.3,冰期后 $^{187}\text{Os}/^{188}\text{Os}$ 初

始值达到了0.5~0.8, 经过Marinoan冰期后又上升到1.2(图5(a)). 其中, 加拿大Mankenzie Mountain地区的Re-Os数据更是完整记录了一个剖面前后2个冰期3个地层的Re-Os同位素年龄及Os初始值变化. 年龄从732.2 Ma 到 662.4 Ma, 再到 632.3 Ma, 对应的 $^{187}\text{Os}/^{188}\text{Os}$ 初始值分别为0.15, 0.54, 1.21. 这说明在冰期前, 海底的热液活动是很剧烈的, 冰期的到来可能使得海底热液的活动减弱, 但同时大陆的风化程度也较弱. 而冰期之后, 随着大陆风化作用的加强, 来自陆地的高放射性成因Os随河水进入到了海水中, 使得 $^{187}\text{Os}/^{188}\text{Os}$ 初始值明显升高, 且同期Sr同位素比值在冰期结束后的迅速升高也说明了风化作用的加强^[45]. 近年关于中、新元古代页岩的研究显示, 对于产自潮缘、泻湖等局限盆地的页岩, 由Re-Os等时线得到的 $^{187}\text{Os}/^{188}\text{Os}$ 初始值要比同时期海相页岩 $^{187}\text{Os}/^{188}\text{Os}$ 初始值偏大一些, 因其更容易受到陆源物质的影响^[34,44].

3.3 大气中O₂含量与 $^{187}\text{Os}/^{188}\text{Os}$ 初始值

大气圈氧化是地球史上最重大的地质事件之一, 它不仅改变了地球表层环境条件、加速了表生地质过程和新矿物的产生, 而且改变了海洋化学条件和元素循环^[46]. 目前研究认为^[47,48], 在显生宙以前, 大气中的氧逸度曾出现过两次快速的上升, 一次是25~20亿年左右的大氧化事件(GOE), 一次是800~600 Ma的新元古代氧化事件(NOE), 经过这两次氧化事件, 大气中的氧含量在500 Ma时基本达到了现在的水平(图5(b)), 并且使得深部大洋发生氧化. 最新研究显示, 相比于微生物的产氧光合作用, 有机质的大量埋

藏可能是使大气氧含量升高的更重要的因素, 碳的埋藏减少了其与氧的结合, 从而使得大气的氧含量能够在新元古代末期较短的时间内迅速升高^[49].

近年来, 针对“大塘坡式”锰矿含锰黑色页岩的主元素、微量元素、稀土元素、硫同位素、碳同位素等的分析显示, 锰质可能主要来源于深部热液^[50~53]. 而新元古代末期氧含量的升高与几次冰期呈现出耦合的关系, 也被认为与“大塘坡式”锰矿的形成有关^[18,54]. 冰期期间, 冰层的覆盖阻隔了海水与大气的物质交换, 使得海水缺氧从而形成了一个铁化甚至硫化的状态^[55], 海底热液活动使得裂谷盆地中出现了大量Mn²⁺. 冰期之后, 随着冰层的消失及大气氧含量的增加, 生物大规模爆发, 表层海水被氧化, Mn²⁺也随之被氧化成MnO₂而发生沉淀, 伴随着有机质的埋藏及成岩过程而被还原成菱锰矿^[56]. 最近有研究^[44]显示, $^{187}\text{Os}/^{188}\text{Os}$ 初始值的升高与当时大气的氧气含量呈耦合关系(图5(b)), 可能因为大气中氧气含量升高, 导致陆地的风化加强, 从而使得高放射性成因的Os随河水进入到了大洋中. 本文所得到的大塘坡组底部黑色页岩的 $^{187}\text{Os}/^{188}\text{Os}$ 初始比值数据, 也说明冰期之后大气氧含量的快速上升, 冰川融水携带着陆源物质进入大塘坡组所在的裂谷盆地, 使得该地区的表层海水快速氧化, 且氧化程度较远洋地带更高, 从而使得锰质在此盆地内发生氧化沉淀, 并在盆地底部的还原环境中伴随着有机碳的埋藏最终被还原进而形成菱锰矿.

4 结论

(1) 贵州道坨锰矿大塘坡组含锰黑色页岩的

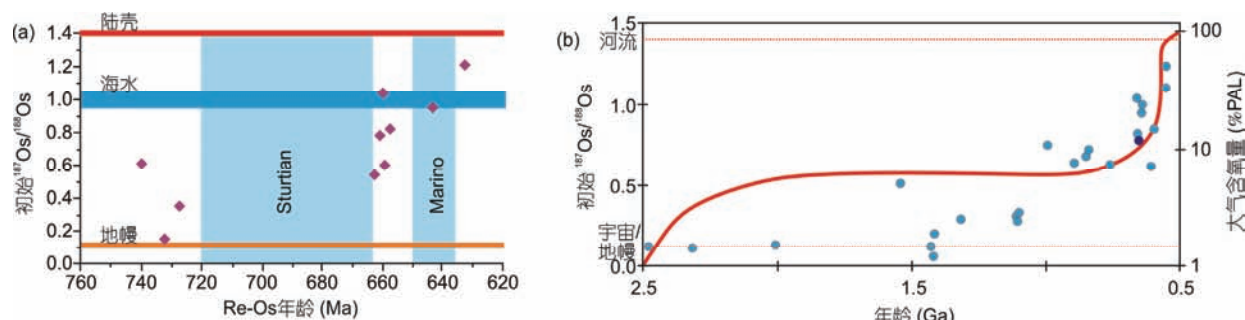


图5 $^{187}\text{Os}/^{188}\text{Os}$ 初始值变化. (a) 全球新元古代冰期前后古海水 $^{187}\text{Os}/^{188}\text{Os}$ 初始值变化(数据来自表2); (b) 元古代海相页岩 $^{187}\text{Os}/^{188}\text{Os}$ 与大气氧含量变化关系^[44](深蓝色点为本文值, 其余点来自文献[44])

Figure 5 Variations of initial $^{187}\text{Os}/^{188}\text{Os}$. (a) The variations of initial $^{187}\text{Os}/^{188}\text{Os}$ of paleo-seawater before and after the global Neoproterozoic glaciation (data from Table 2); (b) temporal variation in Re-Os isochron-derived initial $^{187}\text{Os}/^{188}\text{Os}$ ratio of Proterozoic marine shales^[44] (mazarine pot is from this paper, others from Ref. [44])

Re-Os同位素等时线年龄为 660.6 ± 7.5 Ma, 该年龄与前人测定的大塘坡组底部的凝灰岩中的锆石U-Pb年龄在误差范围内一致, 进一步限定了锰矿的成矿时代和Sturtian冰期的结束年龄, 且可与全球Sturtian冰期结束的Re-Os同位素年龄对比。

(2) 由Re-Os等时线年龄得到的 $^{187}\text{Os}/^{188}\text{Os}$ 初始比

值为0.781, 代表了Sturtian冰期之后的海水值。结合前人的研究, 认为在Sturtian冰期后伴随着大气氧含量的快速升高及陆地冰川的融化, 冰川融水携带着陆源物质进入到含Mn²⁺的裂谷盆地, 使得盆地表层水体含氧量迅速增加, Mn²⁺被氧化为MnO₂而沉淀, 并在底部伴随着有机质的埋藏及成岩作用而最终形成菱锰矿。

致谢 北京大学沈冰教授对英文摘要进行了润色, 国家地质实验测试中心李欣尉助理研究员在溶样方法及讨论方面给予了很大帮助, 两位审稿人提出的问题与建议使得本文的论述更加严谨, 在此一并感谢。

参考文献

- Fairchild I J, Kennedy M J. Neoproterozoic glaciation in the Earth System. *J Geol Soc*, 2007, 164: 895–921
- Kirschvink J L. Late Proterozoic low-latitude global glaciation: The snowball Earth. In: Schopf J W, Klein C, Des Maris D, eds. *The Proterozoic Biosphere: A Multidisciplinary Study*. New York: Cambridge University Press, 1992. 51–52
- Hoffman P F. A neoproterozoic snowball earth. *Science*, 1998, 281: 1342–1346
- Spence G H, Le Heron D P, Fairchild I J. Sedimentological perspectives on climatic, atmospheric and environmental change in the Neoproterozoic Era. *Sedimentology*, 2016, 63: 253–306
- Zhang Q R, Lan Z W. An update on the chronostratigraphy of the Nanhuan System (in Chinese). *J Stratigr*, 2016, 40: 297–301 [张启锐, 兰中伍. 南华系、莲沱组年龄问题的讨论. 地层学杂志, 2016, 40: 297–301]
- Du A D, Qu W J, Wang D H, et al. Rhenium-Osmium Isotope and Its Application in Mineralogy (in Chinese). Beijing: Geological Publishing House, 2012. 110–120 [杜安道, 屈文俊, 王登红, 等. 锑-锇法及其在矿床学中的应用. 北京: 地质出版社, 2012. 110–120]
- Li C, Qu W J, Wang D H, et al. The progress of applying Re-Os isotope to dating of organic-rich sedimentary rocks and reconstruction of palaeoenvironment (in Chinese). *Acta Geosci Sin*, 2014, 35: 405–414 [李超, 屈文俊, 王登红, 等. Re-Os 同位素在沉积地层精确定年及古环境反演中的应用进展. 地球学报, 2014, 35: 405–414]
- Ravizza G, Turekian K K. Application of the $^{187}\text{Re}-^{187}\text{Os}$ system to black shale geochronometry. *Geochim Cosmochim Acta*, 1989, 53: 3257–3262
- Ravizza G, Turekian K K. The osmium isotopic composition of organic-rich marine sediments. *Earth Planet Sci Lett*, 1992, 110: 1–6
- Ravizza G, Eßer B K. A possible link between the seawater osmium isotope record and weathering of ancient sedimentary organic matter. *Chem Geol*, 1993, 107: 255–258
- Cohen A S, Coe A L, Bartlett J M, et al. Precise Re-Os ages of organic-rich mudrocks and the Os isotope composition of Jurassic seawater. *Earth Planet Sci Lett*, 1999, 167: 159–173
- Jaffe L A, Peucker-Ehrenbrink B, Petsch S T. Mobility of rhenium, platinum group elements and organic carbon during black shale weathering. *Earth Planet Sci Lett*, 2002, 198: 339–353
- Li C, Qu W J, Wang D H, et al. Dissolving experimental research of Re-Os isotope system for bitumen samples (in Chinese). *Rock Min Anal*, 2011, 30: 688–694 [李超, 屈文俊, 王登红, 等. 沥青样品铼-锇同位素分析溶解实验研究. 岩矿测试, 2011, 30: 688–694]
- Li C, Qu W J, Wang D H, et al. Research and Preliminary Application of Re-Os isotope system for limestone samples (in Chinese). *Rock Min Anal*, 2011, 30: 259–264 [李超, 屈文俊, 王登红, 等. 石灰岩铼-锇同位素分析方法研究及应用初探. 岩矿测试, 2011, 30: 259–264]
- Peucker-Ehrenbrink B, Ravizza G, Hofmann A W. The marine $^{187}\text{Os}/^{186}\text{Os}$ record of the past 80 million years. *Earth Planet Sci Lett*, 1995, 130: 155–167
- Yang S T, Zhuo X Z, Chen X S, et al. Ore controlling factors of rhodochrosite ore bed from Datangpo Formation in northeast Guizhou (in Chinese). *Miner Depos*, 2016, 35: 1062–1072 [杨胜堂, 蔡喜准, 陈骁帅, 等. 黔东北大塘坡组菱锰矿矿床控矿因素研究. 矿床地质, 2016, 35: 1062–1072]
- Zhu X K, Peng Q Y, Zhang R B, et al. Basic geological and geochemical characteristics of Daotuo super-large manganese ore deposit at Songtao Country in Guizhou Province (in Chinese). *Acta Geol Sin*, 2013, 87: 1335–1348 [朱祥坤, 彭乾云, 张仁彪, 等. 贵州省松桃县道坨超大型锰矿床地质特征. 地质学报, 2013, 87: 1335–1348]
- Zhou Q, Du Y S, Yuan L J, et al. The structure of the Wuling Rift Basin and its control on the manganese deposit during the Nanhua Period in Guizhou-Hunan-Chongqing Border Area, South China (in Chinese). *Earth Sci*, 2016, 41: 177–188 [周琦, 杜远生, 袁良军, 等. 黔湘渝毗邻区南华纪武陵裂谷盆地结构及其对锰矿的控制作用. 地球科学, 2016, 41: 177–188]

- 19 Selby D, Creaser R A. Re-Os geochronology of organic rich sediments: An evaluation of organic matter analysis methods. *Chem Geol*, 2003, 200: 225–240
- 20 Liu H. Study on the method of Re-Os dating for black shale and oil shale (in Chinese). Master Dissertation. Beijing: China University of Geosciences, 2008 [刘华. Re-Os 同位素体系测定黑色页岩、油页岩年龄研究. 硕士学位论文. 北京: 中国地质大学, 2008]
- 21 Yin L, Li J, Zhao P P, et al. A new method for analysis of Re-Os isotopic system in organic-rich sediments (in Chinese). *Geochimica*, 2015, 44: 225–237 [尹露, 李杰, 赵佩佩, 等. 一种新的适合富有机质沉积岩的 Re-Os 同位素分析方法初探. 地球化学, 2015, 44: 225–237]
- 22 Liu H, Qu W J, Wang Y B, et al. Primary study on Re-Os isotopic dating of black shale using CrO₃-H₂SO₄-Carius tube-inductively coupled plasma mass spectrometry system (in Chinese). *Rock Min Anal*, 2008, 27: 245–249 [刘华, 屈文俊, 王英滨, 等. 用三氧化铬-硫酸溶剂对黑色页岩铼-锇定年方法初探. 岩矿测试, 2008, 27: 245–249]
- 23 Du A D, Qu W J, Li C, et al. A review on the development of Re-Os isotopic dating methods and techniques (in Chinese). *Rock Min Anal*, 2009, 28: 288–304 [杜安道, 屈文俊, 李超, 等. 铼-锇同位素定年方法及分析测试技术的进展. 岩矿测试, 2009, 28: 288–304]
- 24 Li C, Qu W J, Wang D H, et al. Advances in the study of the Re-Os isotopic system of organic-rich samples (in Chinese). *Acta Petrol Mineral*, 2010, 29: 421–430 [李超, 屈文俊, 王登红, 等. 富有机质地质样品 Re-Os 同位素体系研究进展. 岩石矿物学杂志, 2010, 29: 421–430]
- 25 Qu W J, Du A D. Highly precise Re-Os dating of molybdenite by ICP-MS with Carius tube sample digestion (in Chinese). *Rock Min Anal*, 2003, 22: 254–257 [屈文俊, 杜安道. 高温密闭溶样电感耦合等离子体质谱准确测定辉钼矿铼-锇地质年龄. 岩矿测试, 2003, 22: 254–257]
- 26 Qu W J, Du A D, Li C, et al. High-precise determination of osmium isotopic ratio in the Jinchuan copper-nickel sulfide ore samples (in Chinese). *Rock Min Anal*, 2009, 28: 219–222 [屈文俊, 杜安道, 李超, 等. 金川铜镍硫化物样品中锇同位素比值的高精度分析. 岩矿测试, 2009, 28: 219–222]
- 27 Creaser R A, Sannigrahi P, Chacko T, et al. Further evaluation of the Re-Os geochronometer in organic-rich sedimentary rocks: A test of hydrocarbon maturation effects in the Exshaw Formation, Western Canada Sedimentary Basin. *Geochim Cosmochim Acta*, 2002, 66: 3441–3452
- 28 Zhou C, Tucker R, Xiao S, et al. New constraints on the ages of Neoproterozoic glaciations in south China. *Geology*, 2004, 32: 437–440
- 29 Yin C Y, Wang Y G, Tang F, et al. SHRIMP II U-Pb zircon date from the Nanhuan Datangpo Formation in Songtao County, Guizhou Province (in Chinese). *Acta Geol Sin*, 2006, 80: 278–285 [尹崇玉, 王砚耕, 唐烽, 等. 贵州松桃南华系大塘坡组凝灰岩锆石 SHRIMP II U-Pb 年龄. 地质学报, 2006, 80: 278–285]
- 30 Rooney A D S J. A Cryogenian chronology: Two long-lasting synchronous Neoproterozoic glaciations. *Geology*, 2015, 43: 459–462
- 31 Kendall B, Creaser R A, Selby D. Re-Os geochronology of postglacial black shales in Australia: Constraints on the timing of “Sturtian” glaciation. *Geology*, 2006, 34: 729–732
- 32 Rooney A D, Chew D M, Selby D. Re-Os geochronology of the Neoproterozoic-Cambrian Dalradian Supergroup of Scotland and Ireland: Implications for Neoproterozoic stratigraphy, glaciations and Re-Os systematics. *Precambrian Res*, 2011, 185: 202–214
- 33 Rooney A D, Macdonald F A, Strauss J V, et al. Re-Os geochronology and coupled Os-Sr isotope constraints on the Sturtian snowball Earth. *Proc Natl Acad Sci USA*, 2014, 111: 51–56
- 34 Strauss J V, Rooney A D, Macdonald F A, et al. 740 Ma vase-shaped microfossils from Yukon, Canada: Implications for Neoproterozoic chronology and biostratigraphy. *Geology*, 2014, 42: 659–662
- 35 Lan Z, Li X, Zhu M, et al. A rapid and synchronous initiation of the wide spread Cryogenian glaciations. *Precambrian Res*, 2014, 255: 401–411
- 36 Ogg J G, Ogg G, Gradstein F M. *A Concise Geologic Time Scale*: 2016. Amsterdam: Elsevier, 2016
- 37 Macdonald F A, Schmitz M D, Crowley J L, et al. Calibrating the cryogenian. *Science*, 2010, 327: 1241–1243
- 38 Peucker-Ehrenbrink B, Ravizza G. The marine osmium isotope record. *Terra Nova*, 2000, 12: 205–219
- 39 Sharma M, Wasserburg G J, Hofmann A W, et al. Himalayan uplift and osmium isotopes in oceans and rivers. *Geochim Cosmochim Acta*, 1999, 63: 4005–4012
- 40 Yang J H, Jiang S Y, Ling H F, et al. Re-Os isotope tracing and dating of black shales and oceanic anoxic events (in Chinese). *Geosci Front*, 2005, 12: 143–150 [杨競红, 蒋少涌, 凌洪飞, 等. 黑色页岩与大洋缺氧事件的 Re-Os 同位素示踪与定年研究. 地学前缘, 2005, 12: 143–150]
- 41 Levasseur S, Birck J, Allègre C J. Direct measurement of femtomoles of osmium and the ¹⁸⁷Os/¹⁸⁶Os ratio in seawater. *Science*, 1998, 282: 272–274
- 42 Hannah J L, Bekker A, Stein H J, et al. Primitive Os and 2316 Ma age for marine shale: Implications for Paleoproterozoic glacial events and the rise of atmospheric oxygen. *Earth Planet Sci Lett*, 2004, 225: 43–52

- 43 Singh S K, Trivedi J R, Krishnaswami S. Re-Os isotope systematics in black shales from the Lesser Himalaya: Their chronology and role in the $^{187}\text{Os}/^{188}\text{Os}$ evolution of seawater. *Geochim Cosmochim Acta*, 1999, 63: 2381–2392
- 44 Tripathy G R, Singh S K. Re-Os depositional age for black shales from the Kaimur Group, Upper Vindhyan, India. *Chem Geol*, 2015, 413: 63–72
- 45 Halverson G P, Wade B P, Hurtgen M T, et al. Neoproterozoic chemostratigraphy. *Precambrian Res*, 2010, 182: 337–350
- 46 Shi X Y, Li Y L, Cao C Q, et al. Life origin, early evolution stages, and ocean environment changes (in Chinese). *Geosci Front*, 2016, 23: 128–139 [史晓颖, 李一良, 曹长群, 等. 生命起源、早期演化阶段与海洋环境演变. 地学前缘, 2016, 23: 128–139]
- 47 Och L M, Shields-Zhou G A. The Neoproterozoic oxygenation event: Environmental perturbations and biogeochemical cycling. *Earth-Sci Rev*, 2012, 110: 26–57
- 48 Mei M X. Great Oxidation Event in history of the Earth: An important clue for the further understanding of evolution of palaeogeographical background (in Chinese). *J Palaeogeogr*, 2016, 18: 315–334 [梅冥相. 地球历史中的巨型氧化作用事件: 了解古地理背景演变的重要线索. 古地理学报, 2016, 18: 315–334]
- 49 Husson J M, Peters S E. Atmospheric oxygenation driven by unsteady growth of the continental sedimentary reservoir. *Earth Planet Sci Lett*, 2017, 460: 68–75
- 50 Yang R D, Gao J B, Cheng M L, et al. Sedimentary geochemistry of manganese deposit of the Neoproterozoic Datangpo Formation in Guizhou Province, China (in Chinese). *Acta Geol Sin*, 2010, 84: 1781–1790 [杨瑞东, 高军波, 程玛莉, 等. 贵州从江高增新元古代大塘坡组锰矿沉积地球化学特征. 地质学报, 2010, 84: 1781–1790]
- 51 He Z W, Yang R D, Gao J B, et al. The geochemical characteristics and sedimentary environment of manganese-bearing rock series of Daotuo manganese deposit, Songtao County of Guizhou Province (in Chinese). *Geol Rev*, 2014, 60: 1061–1075 [何志威, 杨瑞东, 高军波, 等. 贵州松桃道坨锰矿含锰岩系地球化学特征和沉积环境分析. 地质论评, 2014, 60: 1061–1075]
- 52 Yu W, Algeo T J, Du Y, et al. Genesis of Cryogenian Datangpo manganese deposit: Hydrothermal influence and episodic post-glacial ventilation of Nanhua Basin, South China. *Paleogeogr Paleoclimatol Paleoecol*, 2016, 459: 321–337
- 53 Wu C, Zhang Z, Xiao J, et al. Nanhuan manganese deposits within restricted basins of the southeastern Yangtze Platform, China: Constraints from geological and geochemical evidence. *Ore Geol Rev*, 2016, 75: 76–99
- 54 Zhang F F. The formation mechanism of Datangpo manganese ore deposits during Nanhua Period in South China and the paleo-redox conditions of Nanhua Marine Basin (in Chinese). Master Dissertation. Beijing: Chinese Academy of Geological Sciences, 2014 [张飞飞. 华南南华系含锰建造的形成机制与南华纪间冰期海洋的氧化还原状态. 硕士学位论文. 北京: 中国地质科学院, 2014]
- 55 Li C, Love G D, Lyons T W, et al. A stratified redox model for the Ediacaran ocean. *Science*, 2010, 328: 80–83
- 56 Roy S. Sedimentary manganese metallogenesis in response to the evolution of the Earth system. *Earth-Sci Rev*, 2006, 77: 273–305

Summary for “贵州道坨锰矿成矿时代及环境的 Re-Os 同位素证据”

Mineralization age and metallogenic environment of Daotuo manganese deposits in Guizhou: Evidence from Re-Os isotopes

PEI HaoXiang^{1,2}, FU Yong^{3,1*}, LI Chao⁴, LI YanHe^{1,2} & AN ZhengZe⁵

¹ Institute of Mineral Resource, Chinese Academy of Geological Sciences, Beijing 100037, China;

² MLR Key Laboratory of Metallogeny and Mineral Assessment, Beijing 100037, China;

³ College of Resource and Environmental Engineering, Guizhou University, Guiyang 550000, China;

⁴ National Research Center for Geoanalysis, Beijing 100037, China;

⁵ No. 103 Geological Party, Bureau of Geology and Mineral Exploration and Development of Guizhou Province, Tongren 554300, China

* Corresponding author, E-mail: byez1225@126.com

The Neoproterozoic is a critical interval in Earth's history, having witnessed the breakup of supercontinent Rodinia, global glaciations (or the snowball Earth), and the evolution of multicellular organisms. It is proposed that the breakup of Rodinia might have triggered the snowball Earth, while the termination of the Neoproterozoic global glaciations might have triggered the evolution of life in the Ediacaran Period. Two snowball Earth events, the Sturtian (717–663 Ma) and the Marinoan (654–635 Ma) glaciations, were separated by an interglacial interval of ~10 million years (663–654 Ma). In South China, the Sturtian and Marinoan glacial deposits are represented by the Jiangkou and Nantuo Formations. The interglacial Datangpo Formation is characterized by widespread manganese (Mn) ore deposits, such as the Datangpo and Xixibao in Guizhou, Minle in Hunan, and Xiushan in Chongqing, representing the most important metallogenic period of Mn in China.

The Daotuo Mn ore, a superlarge-scale deposit (approximately 200 million tons), was first discovered in 2010 in northeastern Guizhou. It is hosted in a fault-bound depression system between the Yangtze block and the Jiangnan orogenic belt. The Mn ores were discovered in black shale of the Member I of the Datangpo Formation, and occur as rhodochrosite ($MnCO_3$). In order to constrain the age of Mn ores, here we report Re-Os isochron age of the ore-bearing black shale from the Member I of the Datangpo Formation. The Re-Os isochron age of the Member I black shale is 660.6 ± 7.5 Ma, consistent with the zircon U-Pb age of the tuff layer from the base of the Datangpo Formation and other Re-Os isochron ages from other localities (such as Canada, Australia, Scotland, and Mongolia). Furthermore, the initial value of $^{187}\text{Os}/^{188}\text{Os}$ from the Re-Os isochron age is 0.781, suggesting predominantly terrestrial input. Based on previous research, it is shown that during the Sturtian glaciation, under the influence of sea ice cover barrier and atmospheric material exchange, the hypoxic water led to the formation of iron and sulfide rich environments on the seafloor near hydrothermal vents, giving rise to a large number of rift basins rich in Mn^{2+} . After the glaciation and water and atmospheric exchange of material recovery, the glacier meltwater carries the terrigenous material into the rift basin containing Mn^{2+} , accompanied by the melting of the land glacier and the rapid increase of the atmospheric oxygen content. The surface water body of the rift basin is rapidly oxidized, and the oxidation degree is higher than the ocean area. Mn^{2+} are also oxidized to MnO_2 and precipitate back into the environment, where they bury with organic matter, undergo diagenesis, and eventually form rhodochrosite.

manganese deposits, Datangpo Formation, Re-Os isotopes, glaciation

doi: 10.1360/N972017-00450